Ninth International Conference on Computational Fluid Dynamics (ICCFD9), Istanbul, Turkey, July 11-15, 2016

ICCFD9-xxxx

TURBULENT WALL JET OVER A FORWARD-BACKWARD FACING STEP PAIR

Kabache Malika[1] & Mataoui Amina[2]

[1]University of M'Hamed Bouguerra, Boumerdes

[2]Theoretical and applied laboratory of fluid mechanics

Faculty of physics, University of Science and technology HouariBoumedienne, Algiers, Algeria

[1]mkabache@yahoo.com , [2]mataoui_amina@yahoo.fr

Abstract. This study investigates the wall jet outer layer effect on flow structure over obstacle. Indeed, two inlet flow configurations are tested; a turbulent wall jet which has a particular structure with two sources of turbulence production (the first is due to the shear flow associated to the inner layer characterized by small scale and second one is of the free shear jet flow with large turbulence scales) and a free boundary layer flow. The inner region of these two flows is similar, but their external regions are extremely different. The flow structure mainly depends mainly on the momentum of the incoming flow. The secondary eddy of the backward facing step corner appears only in the case of the boundary layer incoming flow. For the two configuration of incoming flow (Boundary layer or Wall jet), the distribution of mean Nusselt number is correlated according with some problem parameters.

Keywords: Separated flow ; Heat transfer ; CFD ; Obstacle , Turbulence

1.Introduction

Turbulent flow over obstacles is a challenging task in heat exchangers, electronic equipments, nuclear reactors and other thermal devices. The channel flow or boundary layer over solid obstacle has been used for these applications by many researchers in the past. Wall jet over obstacle is often found in multi-processor electronic components. Hence it is important to understand this type of flow characteristics. A small number of studies on the wall jet flow over a separated flow are found in the literature ([1-4]).These authors confirm that for the case of a wall jet (b=H), the reattachment length is practically halved compared to that of the boundary layer case. This diminution is explained by the effect of the compression of the external shear layer of the wall jet. The reattachment length of BFS flow in the wall jet case is reduced significantly compared to that of the boundary layer case and they confirmed through the kinetic energy contours that the reduction is due to the turbulent external layer of the wall jet effect on the recirculation zone.The process of separation and reattachment in a turbulent wall jet flow over an obstacle is performed numerically .The effect nozzle thickness and jet exit Reynolds number on the flow structure are investigated. A schematic diagram and parameters of the configuration are shown in Fig. 1.

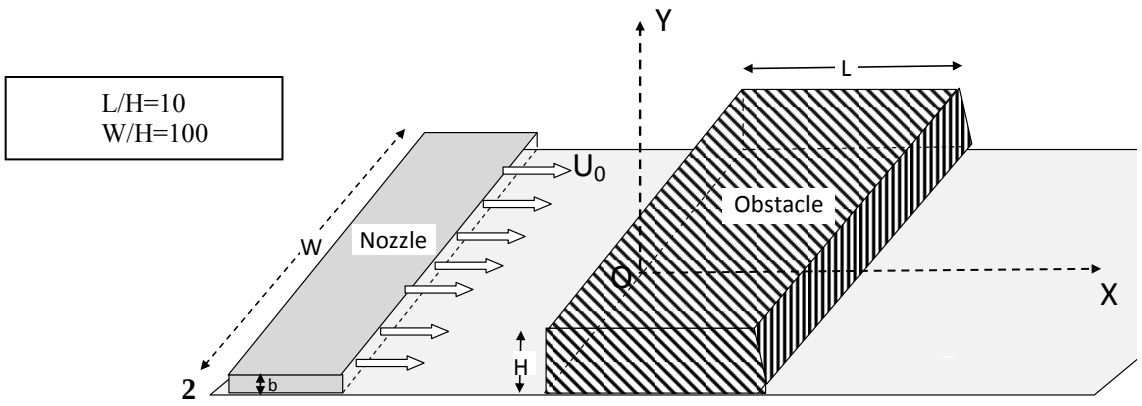

Figure. 1. The geometry of the configuration

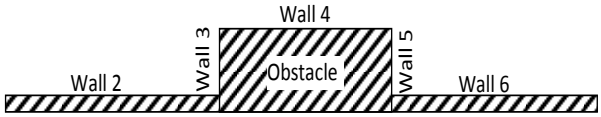

Figure 2. The geometry of the configuration

2.Methodology

2.1 Governing equations

The continuity, Navier-Stokes and energy equations for the steady state incompressible flow are averaged as:

Continuity: $$\frac{\partial U_j}{\partial x_j} = 0 \qquad (1)$$

Momentum: $$U_j \frac{\partial U_i}{\partial x_j} = -\frac{\partial P}{\partial x_i} + \frac{\partial}{\partial x_j}\left[\nu \frac{\partial U_i}{\partial x_j} - \overline{u_i u_j}\right] \quad \text{where } \overline{u_i u_j} = \frac{2}{3}k\delta_{ij} - \nu_t(U_{i,j} + U_{j,i}) \qquad (2)$$

Energy equation: $$U_i \frac{\partial T}{\partial x_i} = \frac{\partial}{\partial x_j}\left(\frac{\nu}{\mathrm{Pr}} \frac{\partial T}{\partial x_j} - \overline{u_j \theta}\right) \qquad (3)$$

where $\overline{u_j \theta} = \Gamma_t \frac{\partial T}{\partial x_j}$

Where U_i is the mean velocity component in x_i direction; T is the mean temperature and u_i is the velocity fluctuation component. θ is the temperature fluctuation, P is the static pressure and ρ is the fluid

density. $\overline{u_i u_j}$ are the Reynolds stress tensor components depending on eddy viscosity $\nu_t = \frac{k}{\omega}$. The quantities $\overline{u_j \theta}$ represent the turbulent heat flux depends on $\Gamma_t = \frac{\nu_t}{\mathrm{Pr}_t}$

3. NUMERICAL PROCEDURE

The finite volume method requires a transformation of the equations in conservative form (Patankar S.V. [6]), to convection, diffusion and source terms. The transport equations are discretized on collocated meshes. The convection and diffusion terms are interpolated using the POWER LAW scheme for all variables, excepting for the pressure where the second order scheme is applied. The pressure–velocity coupling is achieved by SIMPLE algorithm.

3.1 Boundary conditions

The boundaries conditions are sketched in Figure 2 including inflow (Inlet), solid wall, symmetry and outlet conditions, as follows:

- The inlet boundary conditions are chosen as follow:

$U=U_0$, $V=0$, $I_0=k_0/U_0^2$, $\varepsilon_0 = C_\mu \frac{(k_0)^{3/2}}{l_m}$, $\omega_0 = \frac{1}{c_\mu}\frac{\varepsilon_0}{k_0}$, $T=T_0$.

Where C_μ is a turbulence model empirical constant (C_μ=0.09 and l_m is a length scale. For each wall, the non-slip condition is imposed (U=V=0). The kinetic energy (k) is set to zero and the specific of dissipation rate ω corresponds to the asymptotic value proposed by Wilcox [7]. The obstacle walls are maintained at constant temperature ($T_w > T_0$). All other walls of the configuration are adiabatic. For the section BC (see figure 2), the pressure inlet boundary is imposed for the wall jet cases and velocity inlet for boundary layer incoming flow case. At the free boundary, pressure outlet (fully developed) boundary conditions are used. The pressure at outlet boundary conditions is kept at the atmospheric value. At this boundary, the temperature reaches the ambient value ($T=T_0$). Symmetry condition is imposed for the case of boundary incoming flow at the upper horizontal edge.

4. VALIDATION

Figure 3 (a) depicts the normalized velocity U/U_0 versus the dimensionless position y/δ at x=-20H. A good agreement is obtained between the present study and experimental data of Kleebanof [8].
The plane wall jet is characterised by two zones: The inner layer extending from the wall to the section of maximum velocity; analogous to the boundary layer profile and the outer layer that extends from the section of maximum velocity at the outer edge; similar to the free jet profile (Eriksson et al. [9]).
Upstream of the obstacle, at x = -20H, the dimensionless velocity (U/U_{max}) versus the normalised distance ($y/y_{1/2}$) profiles are compared with available experimental data of Eriksson et al [9] (figure 3 (b)). A good agreement is observed between the two predictions. Furthermore, this figure confirms that the impinging flow pattern upstream to the obstacle is a fully developed turbulent wall jet.

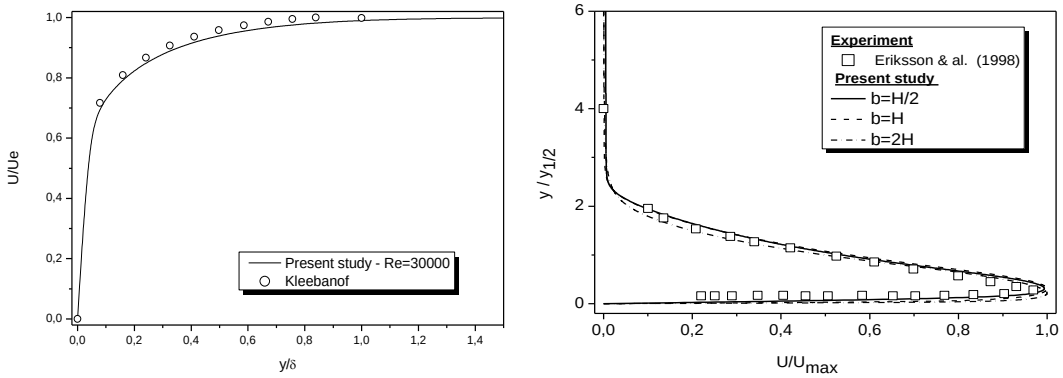

Figure 3. Mean velocity profiles (Re=30000)

The validation case is performed with the available experimental results of B.V. Mudgal and B.S. Pani [10], for a turbulent wall jet over a cube. The figure 4, illustrates the numerical predictions based on the k-ω SST model of the velocity profiles compared to their corresponding experimental data of B.V. Mudgal and B.S. Pani [10]. The measurements are achieved by laser-Doppler anemometer. Sixteen cross-sections are considered. This figure shows an overall good agreement , confirming that the present numerical technique and k-ω SST turbulence model are suitable for this type of flow configuration.

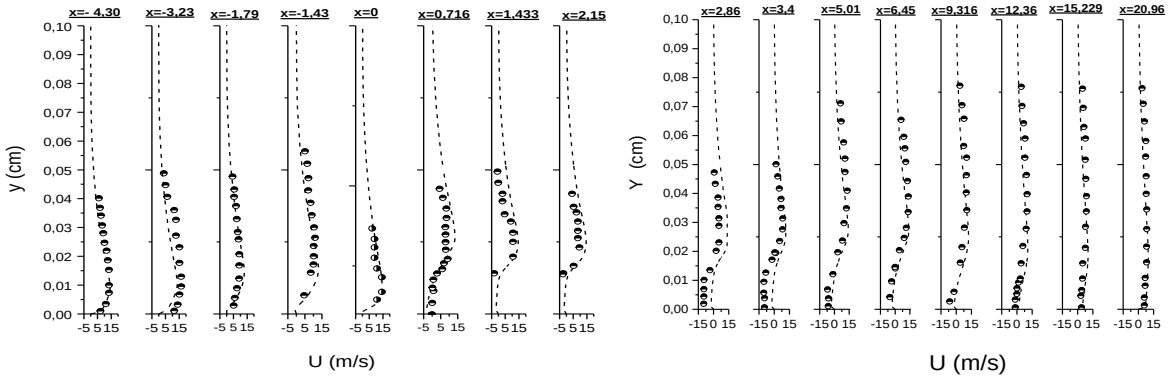

Figure 4. Velocity profile - Validation (H=1cm , L=H , δ/H=0.5, Re=20000)

5. RESULTS

The Shear Stress Tensor k-ω one point closure model is used in this study ([5]). The numerical predictions based on finite volume method are performed by ANSYS FLUENT 14.0 CFD code. The finite volume method requires a transformation of the equations in conservative form ([6]).The convection and diffusion terms are interpolated using the POWER LAW scheme for all variables, except for the pressure where the SECOND ORDER scheme is applied.The pressure–velocity coupling is achieved by the SIMPLE algorithm. As shown in Fig. 2(a), the streamlines of the two types of incoming flow are different. This Figure highlights the interaction of the jet external shear layer with the obstacle. Since, for a given Reynolds number, the momentum of the boundary incoming flow significantly exceeds those of all wall jet incoming flows (Table 1).

Table 1. Momentum of the incoming flow

	Wall jet incoming flow			Boundary layer incoming flow
	b=H/2	b=H	b=2H	
Incoming flow momentum	$J_{H/2}=2\ \rho U^2H$	$J_H\rho\rho U^2H$	$J_{2H}=\rho U^2H/2$	$J_{BL}=\rho U^2h$ where h>10H

To clarity, an enlargement in the obstacle area is performed in figure 2(b). Around the obstacle flow develops three main recirculation zones around the obstacle for each tested case (wall jet (H/2≤b≤H) and boundary layer inlet flow). The nozzle width influences strongly the volume of eddies (Fig. 2(b)). For the Boundary layer incoming flow, the first eddy (forward facing step and the third eddy (backward facing step) have the largest size; contrary to that of the second eddies (atop of the obstacle) which is reduced in comparison to that of the wall jet incoming flow. The reattachment length of the first and the third eddy increase when the nozzle thickness increases, the highest value is obtained for the boundary layer incoming flow. Inversely to the second bubble, the reattachment length decreases when the nozzle thickness increases and the smallest length is obtained for the boundary layer case. The secondary eddy of the backward facing step corner appears only in the case of the boundary layer incoming flow. The flow structure mainly depends on the incoming flow parameters particularly the momentum of the incoming flow (Table 1).

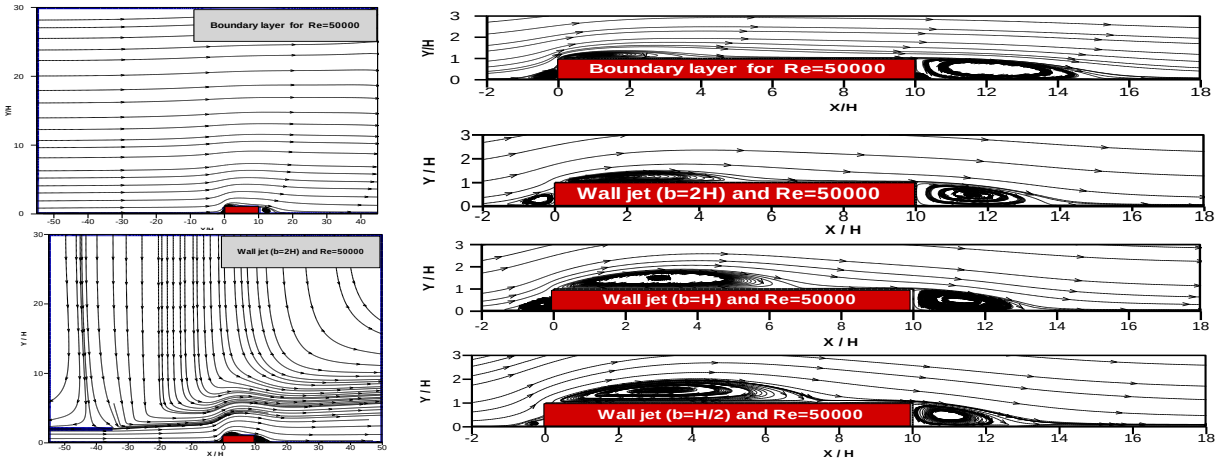

(a) Effect of incoming flow configuration (b) Effect of incoming flow configuration and wall jet thickness

Figure. 5 Streamlines contours (L/H=10 and W/H=100)

The turbulence kinetic energy is found high around the nozzle cross section where the shear layer attains the high deformation (Figure. 6). An additional bubble is visible for the cases of the wall jet incoming flow. An alternative description of the turbulent flow field has been obtained using a frequency analysis of the flow instead of measuring the correlation functions. This approach allows a detailed picture of the energy distribution among eddies of different sizes. It plays a significant role in the reattachment process, compressing the eddies, inducing a smaller reattachment length.

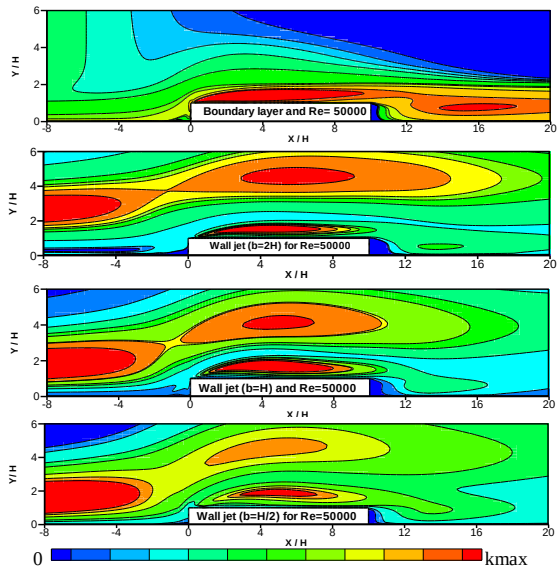

Fig. 6. Contours of kinetic energy

In order to predict the heat transfer rate along the heated walls composing the obstacle, the local Nusselt number is deduced from the temperature distribution. It is defined by Eq. 4:

$$Nu = -\frac{L}{T_w - T_0}\frac{\partial T}{\partial n} \tag{4}$$

Where n is the perpendicular direction to the corresponding wall and L is the length

The average Nusselt number along the heated wall is deduced from Eq. 5:

$$\overline{Nu}_{wall} = \frac{1}{L_{wall}}\int_0^{L_{wall}} Nu\ dl \tag{5}$$

The mean Nusselt number along the walls that form the obstacle is deduced from eq 6. The weighting factor of each term is proportional to each wall length L such as:

$$Nu_{mean} = \frac{L_2\overline{Nu}_{wall2} + L_3\overline{Nu}_{wall3} + L_4\overline{Nu}_{wall4}}{(L_2 + L_3 + L_4)} = \frac{\overline{Nu}_{wall2} + 10\overline{Nu}_{wall3} + \overline{Nu}_{wall4}}{12} \tag{6}$$

Where L_2, L_3 andL_4 are the length of the heated wall (L_2= L_4=H and L_3=10H).

Fig. 4 reflects the effect of the nozzle thickness of the wall jet incoming flow, on heat transfer via the value of average Nusselt number of the obstacle. Based on Fig. 4, the mean Nusselt number over the obstacle is correlated according the parameters of this study, for each incoming flow configuration:

Boundary layer flow: $\overline{Nu}_{mean} = 0.32\ \mathrm{Re}^{0.73}$ (7)

Wall jet flow: $\overline{Nu}_{mean} = \left[0.33 - 0.085\left(\frac{b}{H}\right)\right]\mathrm{Re}^{0.73}$ (8)

Figure.7 evidences the effect of the incoming flow configuration on heat transfer via the value of mean Nusselt number. This could be used from an engineering viewpoint for the purpose of heat transfer enhancement. The wall jets thickness is set for various values and it emerges that the thinnest exhibits the higher heat transfer on each wall of the obstacle and for the entire surface of the obstacle. The boundary

layer case exhibits the higher heat transfer the wall jet cases, because the corresponding momentum of the inlet flow over the obstacle is highest. The convective heat transfer depends mainly on the momentum of the flow.

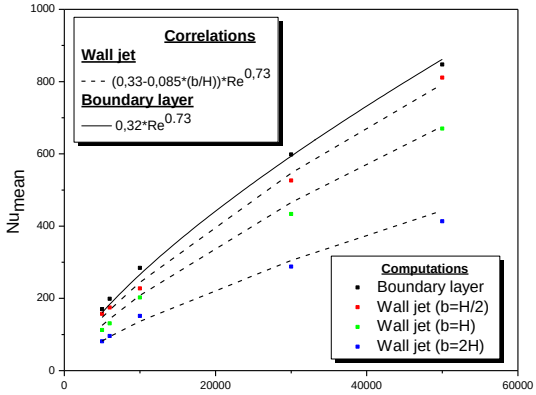

Fig. 7. Mean Nusselt number - Correlations

4. CONCLUSION

This paper examines a separated reattaching flow over a rectangular obstacle. Turbulent eddying zones were identified and controlled by different sources of turbulence: two main shear production sources located on each side of the jet axis and a minor one due to reverse flow inside the recirculation bubble. The reattachment length of the first and the third eddy increase when the nozzle thickness increases, the highest value is obtained for the boundary layer incoming flow. Inversely to the second bubble, the reattachment length decreases when the nozzle thickness increases and the smallest length is obtained for the boundary layer case.

5. References

.

[1] Badri Kusuma, M. S. (1993). Etude expérimentale d'un écoulement turbulent en aval d'une marche descendante: cas d'un jet pariétal et de la couche limite (Doctoral dissertation).

[2] Arous, M., Mataoui, A., & Bouahmed, Z. (2011). Influence of upstream flow characteristics on the reattachment phenomenon in shallow cavities. Thermal science, 15(3), 721-734.

[3] Madi Arous, F., Mataoui, A., Terfous, A., & Ghenaim, A. (2012). Jet–cavity interaction: effect of the cavity depth. Progress in Computational Fluid Dynamics, an International Journal, 12(5), 322-332.

[4] Nait Bouda, N., Schiestel, R., Mataoui, A., Rey, C., and Benabid (2009) . Influence of incoming flow structure on reattachment over a backward facing step. Modelling, Measurement and Control;B Mechanics and Thermics AMSE journal ; Vol. 78 | Issue1 |.

[5] Menter, F. R. (1994). Two-equation eddy-viscosity turbulence models for engineering applications. AIAA journal, 32(8), 1598-1605.

[6] Patankar, S.V. 1980. Numerical heat transfer and fluid flow, Series in computational methods in mechanics and thermal sciences, hemisphere Publishing Corporation.

[7] D. C. Wilcox. Turbulence Modelling for CFD, DCW Industries Inc, La Canada, CA, 1994.

[8] Klebanoff, P. S., & Diehl, Z. W. (1952). Some features of artificially thickened fully developed turbulent boundary layers with zero pressure gradient.

[9] Eriksson, J. G., Karlsson, R. I., & Persson, J. (1998). An experimental study of a two-dimensional plane turbulent wall jet. Experiments in fluids, 25(1), 50-60.

[10] Mudgal, B. V., & Pani, B. S. (1998). Flow around obstacles in plane turbulent wall jets. Journal of Wind Engineering and Industrial Aerodynamics, 73(3), 193-213.